J. Biomedical Science and Engineering, 2015, 8, 429-440
Published Online July 2015 in SciRes. http://www.scirp.org/journal/jbise
http://dx.doi.org/10.4236/jbise.2015.87040

Scientific Research Publishing

A Persistent Na^+ Current and Its Contribution to Burst-Like Firing in Ventral Tegmental Area Dopamine Neurons

Susumu Koyama[1,2*], Munechika Enjoji[2], Mark S. Brodie[1], Sarah B. Appel[1]

[1]Department of Physiology and Biophysics, University of Illinois at Chicago, College of Medicine, Chicago, IL, USA
[2]Department of Clinical Pharmacology, Faculty of Pharmaceutical Sciences, Fukuoka University, Fukuoka, Japan
Email: *susumuk@fukuoka-u.ac.jp

Received 21 November 2014; accepted 9 July 2015; published 13 July 2015

Abstract

The ventral tegmental area dopamine (DA VTA) neurons have the spontaneous tonic activity and an alteration of firing pattern from tonic to burst accelerates dopamine transmission more effectively in the mesoaccumbal dopaminergic system, leading to the reinforcing process of drugs of abuse such as alcohol and nicotine. In the present study, we examined whether a persistent Na^+ current would contribute to burst firing in DA VTA neuronsusing nystatin-perforated recording. Tetrodotoxin (TTX) (1 μM) or riluzole (10 μM) hyperpolarized the membrane potential and stopped spontaneous firing of DA VTA neurons. In voltage-clamp analysis, a TTX and riluzole-sensitive and persistent Na^+ current was activated at −60 mV and reached maximal amplitude at −40 mV. This persistent Na^+ current was potentiated by a negative shift of the voltage of activation by eliminating Ca^{2+} from the extracellular solution. The Ca^{2+}-free extracellular solution depolarized the membrane potential and increased the firing frequency of DA VTA neurons. When a continuous hyperpolarizing current was injected, the firing pattern of the DA VTA neurons transformed into burst-like firing; with average spike number of 4.9, average inter-spike interval of 221 ms, and an average plateau potential, on which the train of spikes generated, was 11 mV. The burst-like firing of DA VTA neurons was abolished by 10 μM riluzole. The concurrent blockade of both T-type Ca^{2+} current and small conductance Ca^{2+}-activated K^+(SK) currents by 100 μM nickel did not induce burst-like firing with or without continuous hyperpolarizing current injection in DA VTA neurons. In conclusion, increases in a persistent Na^+ current that mediates a depolarizing driving force by removing extracellular Ca^{2+} contributes to burst-like firing in DA VTA neurons.

*Corresponding author.

How to cite this paper: Koyama, S., Enjoji, M., Brodie, M.S. and Appel, S.B. (2015) A Persistent Na^+ Current and Its Contribution to Burst-Like Firing in Ventral Tegmental Area Dopamine Neurons. *J. Biomedical Science and Engineering*, **8**, 429-440.
http://dx.doi.org/10.4236/jbise.2015.87040

Keywords

Apamin, Acutely Dissociated Neurons, Extracellular Ca^{2+}, Nickel, Nystatin, Perforated Patch Recording

1. Introduction

Ventral tegmental area dopamine (DA VTA) neurons project their axons to the nucleus accumbens (NAcb) [1]. Increases in the activity of mesoaccumbal dopamine system in the brain are critical for the reinforcing effects of drugs of abuse, such as ethanol and nicotine [2]-[5]. DA VTA neurons have spontaneous rhythmic activity [6]-[10] and the spontaneous activity of midbrain dopamine neurons regulates dopamine release [11]. DA VTA neurons *in vivo* exhibit burst firing in addition to regular and irregular firing patterns [12]-[14] and burst firing accelerates dopamine release from dopaminergic nerve terminals more effectively than tonic firing [15] [16]. Therefore, the transformation of tonic firing into burst firing in DA VTA neurons likely contributes to reinforcing processes mediatedvia the mesoaccumbal dopamine system.

The properties of burst firing have been studied in midbrain dopamine neurons *in vitro* (brain slice preparations) as well as *in vivo* [17] [18]. Both excitatory synaptic activity and intrinsic ionic mechanisms are considered to contribute to the burst firing of DA VTA neurons. DA VTA neurons receive extensive glutamatergic excitatory synaptic afferents from the prefrontal cortex [19] and the burst firing of midbrain dopamine neurons is induced by the activation of N-methyl-D-aspartic acid (NMDA) receptors on these neurons [18] [20]-[23]. The burst firing of midbrain dopamine neurons also depends on two major ion channels: voltage-dependent Ca^{2+} channels and small conductance Ca^{2+}-activated K^+ (SK) channels. Voltage-dependent L-type Ca^{2+} channels mediate the main depolarizing driving force of spontaneous oscillatory potentials (SOPs), which is around 0.5 Hz, and contribute to the subsequent generation of action potentials (APs) [24]-[26]. A previous study reported that blockade of L-type Ca^{2+} channels prevents carbachol-induced burst firing in DA VTA neurons [27]. It has been reported that the inhibition of SK current induces burst firing in midbrain dopamine neurons [28] [29]. A previous study reported that concurrent blockade of T-type Ca^{2+} channels and SK channels by Ni^{2+} induces burst firing in a subset of midbrain dopamine neurons [30]. Taken together, it is likely that L-type Ca^{2+} current contributes to the depolarizing driving force that induces burst firing and the SK current counters this L-type Ca^{2+} channel-mediated depolarizing driving force to prevent burst firing in midbrain dopamine neurons.

Persistent Na^+ currents play a critical role in AP generation in neocortical neurons [31] [32], hippocampal neurons [33] [34], amygdala neurons [35], striatal neurons [36], supraoptic neurons [37], tuberomammillary neurons [38], trigeminal neurons [39], dorsal column neurons [40] and dorsal root ganglion neurons [41]. A recent study has reported that persistent Na^+ currents contribute to the initiation of AP generation in midbrain dopamine neurons [42]. It is well known that the potentiation of persistent Na^+ currents induces burst firing in neurons, as demonstrated by experimental procedures such as modulation of Na^+ channels by phosphorylation [43]-[45], anemone toxin treatment [46], or by reduction of extracellular Ca^{2+} concentrations [47] [48]. Therefore, persistent Na^+ currents may generate burst firing in neurons. In midbrain dopamine neurons, Ca^{2+} current-dependent burst firing has been studied as described above, whereas the properties of Na^+ current-dependent burst firing have not been well studied. In the present study, we examined the properties of a persistent Na^+ current and whether this current contributes to burst firing in DA VTA neurons.

2. Materials and Methods

2.1. Perspective of the Experiments

All electrophysiological experiments in the current study were conducted using a patch-clamp experimental system in the Department of Physiology and Biophysics, University of Illinois at Chicago from 2005 to 2006.

2.2. Preparation of Dissociated Neurons

Animals used in this study were treated in strict accordance with the American Physiological Society's Guiding Principles in the Care and Use of Animals and the U.S. National Institutes for Health Guide for the Care and

Use of Laboratory Animals. The protocol for all experimental methods was approved by the Institutional Animal Care Committee of the University of Illinois at Chicago. Fisher rats (F-344; 14 - 18 days old; male and female) were decapitated and the brains quickly removed. The brains were placed in an ice-cold cutting solution (in mM: 220 sucrose, 2.5 KCl, 2.4 $CaCl_2$, 1.3 $MgSO_4$, 1.24 NaH_2PO_4, 26 $NaHCO_3$ and 11$_D$-glucose), which was constantly bubbled with 95% O_2 and 5% CO_2. Transverse brain slices (400 μm thick) were made on a Vibratome (Series 1000 plus, St. Louis, MO). Brain slices were incubated for 30 min in artificial cerebrospinal fluid (ACSF) (in mM: 126 NaCl, 2.5 KCl, 2.4 $CaCl_2$, 1.3 $MgSO_4$ 1.24 NaH_2PO_4, 26 $NaHCO_3$ and 11 $_D$-glucose; osmolarity 300 mOsm), which was constantly bubbled with 95% O_2 and 5% CO_2 at room temperature (23˚C - 25˚C). The brain slices were then incubated in a HEPES-buffered external solution (see the next section) containing papain (15 - 18 U/ml) at 32˚C - 36˚C for 20 - 26 min. After papain treatment, the brain slices were further incubated in ACSF for 20 - 40 min. VTA neurons were dissociated with a vibrating stylus apparatus for dispersing cells from the brain slices as previously described [9]. Once the cell dissociation procedure was completed (4 - 7 min), the brain slice was removed from the culture dish, and the dissociated neurons usually settled and adhered to the bottom of the dish within 20 min.

2.3. Nystatin-Perforated Patch Recording

In current-clamp recording, nystatin-perforated patch recording was employed as previously described [8]. Microelectrodes were fabricated on a P-87 puller (Sutter Instrument Company, Novato, CA) from glass capillaries (LE16; Dagan, Minneapolis, MN) and heat-polished on a microforge (Narishige, Tokyo, Japan). The tip resistances of the electrodes were 1.5 - 3 MΩ when filled with pipette solution (in mM: 60 K-acetate, 60 KCl, 1 $CaCl_2$, 2 $MgCl_2$ and 40 HEPES; pH adjusted to 7.2 with KOH, final $[K^+]_i$ = 131 mM; 290 mOsm). Nystatin was dissolved in methanol at a concentration of 10 mg/ml. This nystatin stock solution was diluted with pipette solution to a final concentration of 100 - 200 μg/ml and the electrodes were backfilled with this solution. A HEPES-buffered extracellular solution contained (in mM) 145 NaCl, 2.5 KCl, 2 $CaCl_2$, 1 $MgCl_2$, 10 HEPES and 11$_D$-glucose. The pH was adjusted to 7.4 with NaOH and the osmolarity was 310 mOsm. The HEPES-buffered solution was constantly bubbled with 100% O_2. In some experiments, recording was done in a Ca^{2+}-free external solution, in which Ca^{2+} was replaced by equimolar Mg^{2+} to block Ca^{2+} current. The liquid junction potentials between the pipette and extracellular solutions were estimated to be 5 mV [49] and the results have been corrected by this amount. The osmolarity of the solutions was measured by a Vaprovapor pressure osmometer (Wescor Inc., Logan, UT). Electrophysiological measurements were performed using an Axopatch-1B patch clamp amplifier (Axon Instruments, Union City, CA). Membrane currents and voltage were filtered at 1 kHz and acquired at a sampling frequency of 10 kHz. Data acquisition was performed by a DigiData 1322A interface and pClamp software version 9.0 (Axon Instruments). The dissociated VTA neurons were visualized under phase-contrast on an inverted microscope (Diaphot 300, Nikon, Tokyo, Japan). All experiments were performed at room temperature (23˚C - 25˚C).

2.4. Conventional Whole-Cell Recording

In voltage-clamp recording of persistent Na^+ currents, conventional whole-cell recording was employed with the pipette solution (in mM: 60 Cs-methanesulfonate, 80 CsCl, 5 tetraethylammonium (TEA)-Cl, 4 MgATP, 0.3 Na_2GTP, 5 EGTA and 20 HEPES; pH adjusted to 7.2 with Tris-OH; 310 mOsm). The extracellular solution to record persistent Na^+ current contained (in mM) 100 NaCl, 40 TEA-Cl, 5 KCl, 2 $CaCl_2$, 1 $MgCl_2$, 1 $BaCl_2$, 1 CsCl, 0.2 $CdCl_2$, 0.1 $NiCl_2$, 10 HEPES and 11$_D$-glucose. The pH was adjusted to 7.4 with Tris-OH and the osmolarity was adjusted to 320 mOsm with sucrose. The extracellular solution was constantly bubbled with 100% O_2. In some experiments, recording was done in a Ca^{2+}-free external solution, in which Ca^{2+} was replaced by an equimolar Mg^{2+}. The liquid junction potentials between the pipette and extracellular solutions were estimated to be 8 mV and the results have been corrected by this amount.

2.5. Drug Application

Neurons were continuously bathed in the external solution and drugs were dissolved at their final concentration in the same solution. Drug solutions were applied via a multiple channel manifold (MLF-4; ALA Scientific Instruments, Westbury, NY). Each channel of the manifold was connected to a gravity-fed reservoir with tubing

(860 μm, i.d.). The output of the manifold was connected to an outflow tube (500 μm, i.d.), the tip of which was placed within 200 μm of the soma of the recorded neuron. Solution flowed continuously through one manifold channel. Application of drug solutions was controlled by opening or closing valves connected to the reservoirs.

2.6. Source of Drugs and Chemical Agents

The following drugs and chemical agents were used in this study, apamin, $BaCl_2$, CsCl, $CdCl_2$, EGTA, HEPES, nystatin, riluzole, TEA-Cl and tetrodotoxin (TTX) were purchased from Sigma–Aldrich (Saint Louis, MO). Papain was purchased from Worthington (Lakewood, NJ). Riluzole was dissolved in dimethyl sulphoxide (DMSO) and made as a stock solution at a concentration of 100 mM. The stock solution for riluzole was diluted in the HEPES-buffered external solution. The final concentration of DMSO in the HEPES-buffered external solution was 0.01%.

2.7. Data Analysis

Action potentials (APs) were analyzed offline with pClamp 9.0 software (Axon Instruments Inc.). To assess the change of spontaneous firing with drugs, a 60-s-long segment during the peak of the drug response was analyzed as previously described [50]. Inter-spike interval (ISI) histograms were created as previously described [51]. The number of bins was equal to the square root of the number of ISIs. Bin width was obtained by dividing the ISI range (maximum ISI minus minimum ISI) by the number of bins. The coefficient of variation (CV) of the events was obtained by dividing the standard deviation of the event intervals by the mean event intervals. Burst duration was measured between the first spike and the last spike of a spike train. The ISI during burst-like firing was obtained by dividing the burst duration by the number of spike intervals in the burst spike train. The plateau potential, on which the trains of spikes were generated, was measured from the bottom of membrane potential to the threshold of the first spike. The data from cells with AP amplitudes less than 50 mV were discarded. All average values are expressed as mean ± standard error of the mean (S.E.M.). Statistical comparison to assess significant differences was done by the paired or unpaired Student's *t*-test. To analyze persistent Na^+ current activation, the current was normalized to the maximal current and fitted by the Boltzmann equation, using Origin software version 7 (Origin Lab, Northampton, MA):

$$y = A_2 + \left(A_1 - A_2\right) \Big/ \left\{1 + exp\left(x - x_0\right) \Big/ dx\right\}$$

where y is the current at the test voltage of x, A_1 is the minimal current and set to be 0, A_2 is the maximal current and set to be 1, x_0 is the membrane potential for half-activation and dx is the slope factor.

3. Results

3.1. Na^+ Current Contribution to Spontaneous Firing of DA VTA Neurons

Figure 1(A) shows typical spontaneous membrane activity before, during, and after the application of 1 μM TTX in DA VTA neurons. Before TTX treatment, the DA VTA neuron exhibited spontaneous firing (**Figure 1(A)-a**). TTX hyperpolarized the membrane potential and abolished spontaneous firing (**Figure 1(A)-b**). After the washout of TTX, AP generation reappeared (**Figure 1(A)-c**). **Figure 1(B)** shows typical spontaneous membrane activity before, during, and after the application of 10 μM riluzole, a voltage-dependent Na^+ channel antagonist, in DA VTA neurons. Before riluzole treatment, the DA VTA neuron exhibited spontaneous firing (**Figure 1(B)-a**). Riluzole hyperpolarized the membrane potential and abolished spontaneous firing (**Figure 1(B)-b**). After the washout of riluzole, AP generation reappeared (**Figure 1(B)-c**).

3.2. TTX-and Riluzole-Sensitive Persistent Na^+ Currents

To ascertain the presence of persistent Na^+ currents in DA VTA neurons, we used a ramp-voltage protocol with potassium-based pipette solutions and physiological extracellular solutions **Figure 2(A_1)** shows typical currents before and after treatment with 1 μM TTX and TTX-sensitive currents were obtained by the digital subtraction of TTX-insensitive currents from control currents. **Figure 2(B_1)** shows typical currents before and after treatment with 10 μM riluzole and riluzole-sensitive currents were obtained by the digital subtraction of the riluzole-insensitive currents from control currents. The riluzole-sensitive inward current provided a similar current-

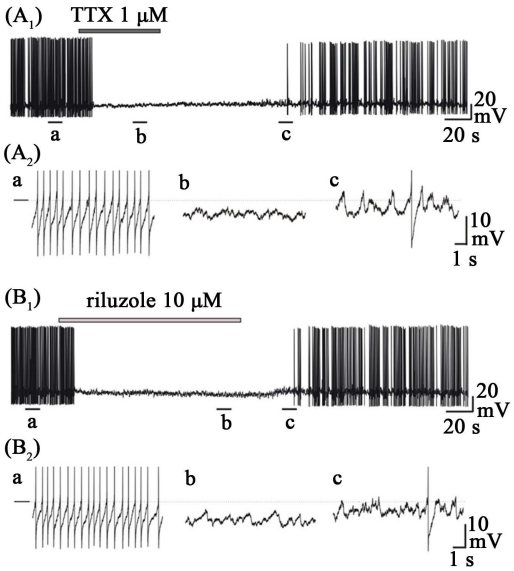

Figure 1. The effects of TTX and riluzole on spontaneous firing in DA VTA neurons. (A_1) Spontaneous membrane activity before, during, and after application of 1 μM TTX in a representative DA VTA neuron. No current was injected; (A_2) 10-s segments from the longer record shown in A_1. Spontaneous activity shown using a faster time scale before (a), during (b), and after treatment with 1 μM TTX (c); (B_1) Spontaneous membrane activity before, during, and after application of 10 μM riluzole in a representative DA VTA neuron. No current was injected; (B_2) 10-s segments from the longer record shown in B_1. Spontaneous activity in a faster time scale before (a), during (b), and after the treatment with 10 μM riluzole (c). A horizontal bar and a dashed line represent the membrane potential of −40 mV.

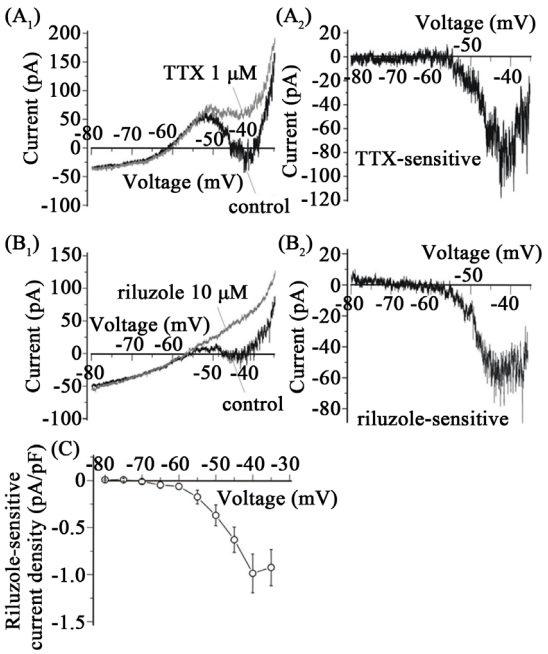

Figure 2. Persistent Na^+ currents of DA VTA neurons. (A_1) Voltage-ramp induced currents before (*black line*) and after (*grey line*) treatment with 1 μM TTX in a representative DA VTA neuron. (*inset*) Slow depolarizing voltage ramp was applied from −90 mV to −10 mV in 2 s (40 mV/s); (A_2) TTX-sensitive current obtained by the digital subtraction of TTX-insensitive current from control current; (B_1) Voltage-ramp induced currents before (*black line*) and after (*grey line*) treatment with 10 μM riluzole in a DA VTA neuron; (B_2) Riluzole-sensitive current obtained by the digital subtraction of riluzole-insensitive current from control current. *C*, Current density-voltage relationship of riluzole-sensitive current in DA VTA neurons (n = 6). Values represent the mean ± SEM.

voltage relationship to the TTX-sensitive current. **Figure 2(C)** shows the current density-voltage relationship of riluzole-sensitive currents in DA VTA neurons.

3.3. Potentiation of Persistent Na^+ Currents with Ca^{2+}-Free Extracellular Solution

We next examined the current-voltage relationship of persistent Na^+ current by a voltage-step protocol using cesium-based pipette solution. To identify DA VTA neurons, cell-attached recording was performed before making conventional whole-cell configuration. In the 6 DA VTA neurons examined, average spontaneous firing frequency was 1.5 ± 0.2 Hz. **Figure 3(A_1)** shows currents induced by the voltage-step protocol before and after application of 2 μM TTX in the control extracellular solution. **Figure 3(A_2)** shows currents induced by the voltage-step protocol before and after application of 2 μM TTX in the Ca^{2+}-free extracellular solution. The graph in

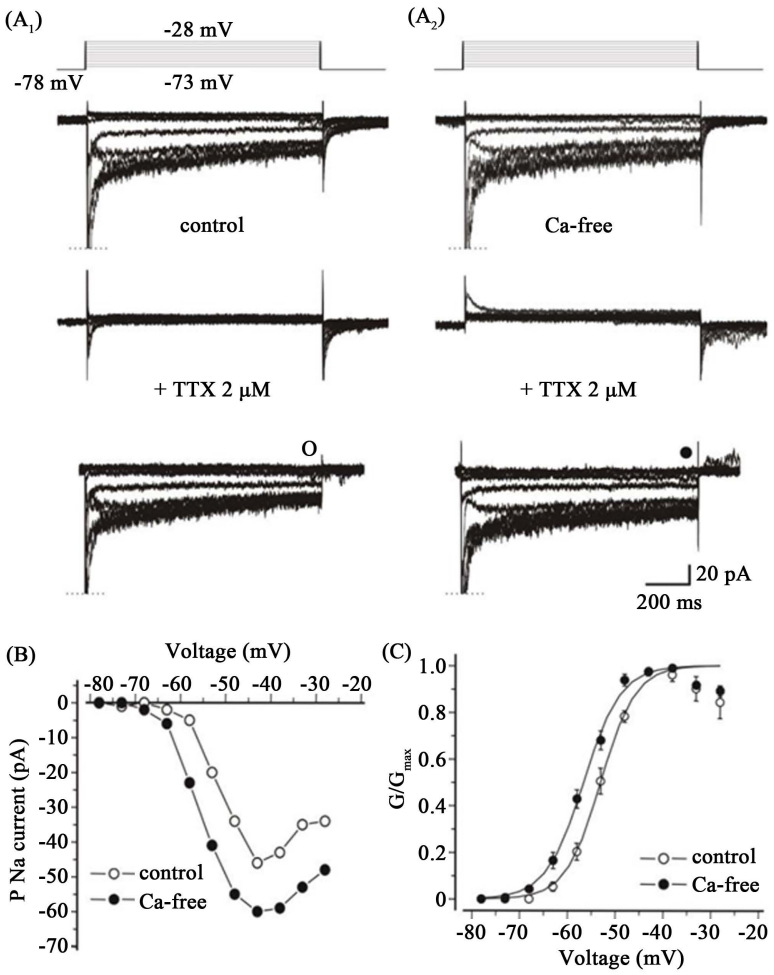

Figure 3. The potentiation of persistent Na^+ currents in Ca^{2+}-free extracellular solution. (A_1) Currents induced in a representative DA VTA neuron before (*top*) and after 2 μM TTX treatment (*middle*) in a normal extracellular solution. TTX-sensitive currents were obtained by the digital subtraction of TTX-insensitive currents from control currents (*bottom*); (A_2) Currents induced in the same DA VTA neuron before (*top*) and after 2 μM TTX treatment (*middle*) in Ca^{2+}-free extracellular solution. TTX-sensitive currents obtained by the digital subtraction of TTX-insensitive currents from control currents in a Ca^{2+}-free extracellular solution (*bottom*). One-second depolarizing voltage steps were applied from a holding potential of −78 mV to −28 mV in 10 mV increments. Persistent Na^+ currents were measured at 100 ms before the end of depolarizing voltage steps (*open and filled circles*). Transient Na^+ currents are truncated; (B) Current-voltage relationship of TTX-sensitive persistent Na^+ currents in the normal extracellular solution (*open circles*) and the Ca^{2+}-free extracellular solution (*filled circles*) (n = 6); (C) Normalized persistent Na^+ currents plotted as a function of test voltage before (*open circles*) and after the elimination of Ca^{2+} from extracellular solutions (*filled circles*) (n = 6). Values represent the mean ± SEM.

Figure 3(B) shows the current-voltage relationship of TTX-sensitive persistent Na^+ currents in the control extracellular solution and the Ca^{2+}-free extracellular solution. **Figure 3(C)** shows the normalized persistent Na^+ current plotted as a function of test voltage before and after the elimination of Ca^{2+} from the extracellular solutions. In the control extracellular solution, average half-activating voltage ($V_{act,\,0.5}$) was −53.6 ± 0.7 mV and average slope factor was 3.4 ± 0.2 (n = 6). In the Ca^{2+}-free extracellular solution, average $V_{act,\,0.5}$ was −57.1 ± 0.7 mV and average slope factor was 3.7 ± 0.2 (n = 6). The elimination of Ca^{2+} from the extracellular solution significantly shifted the $V_{act,\,0.5}$ in a negative direction ($P < 0.001$) without changing the slope.

3.4. Na^+ Current Contribution to Burst-Like Firing

We examined the effect of Ca^{2+}-free extracellular solution, which potentiated persistent Na^+ current, on the firing of DA VTA neurons. **Figure 4(A_1)** shows typical membrane activity before, during, and after the application of Ca^{2+}-free extracellular solution with or without continuous hyperpolarizing current injection. In the control extracellular solution, the spontaneous firing frequency was 1.6 Hz (**Figure 4(A_2)**, a). The Ca^{2+}-free extracellular solution depolarized the membrane potential and increased the firing frequency to 7.6 Hz (**Figure 4(A_2)**, b). When a continuous hyperpolarizing current was injected to counter the depolarizing driving force, burst-like firing was generated in the Ca^{2+}-free extracellular solution (**Figure 4(A_2)**, c). When the continuous hyperpolarizing current injection was removed and the Ca^{2+}-free extracellular solution was switched to the control extra-

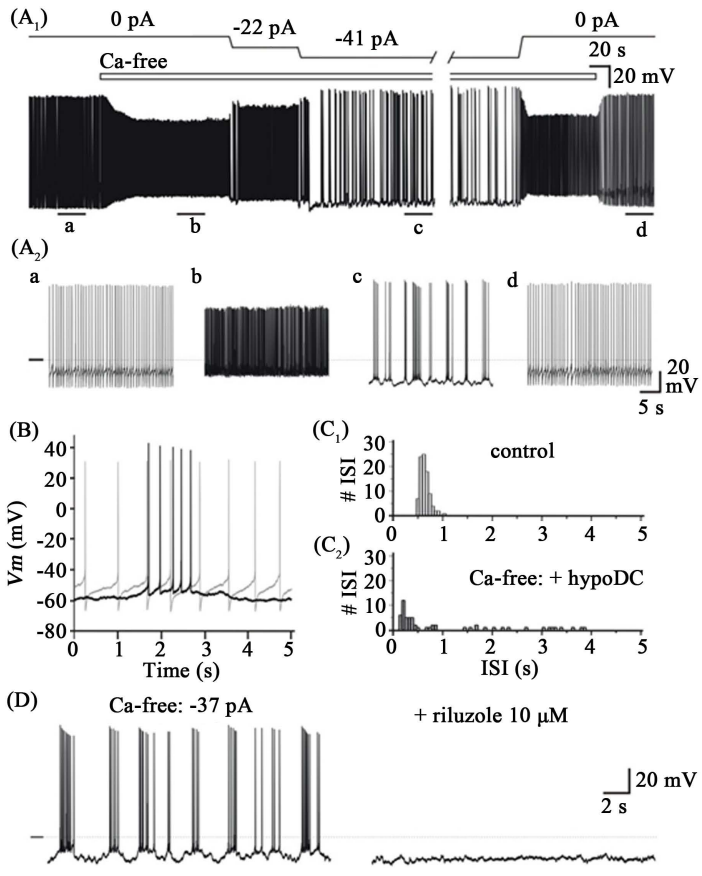

Figure 4. Burst firing of DA VTA neurons. (A_1) Membrane activity before, during, and after the application of Ca^{2+}-free extracellular solution with or without continuous hyperpolarizing current injection in a representative DA VTA neuron; (A_2) 30-s segments from the longer recording shown in A_1. Firing patterns in the control (a), in the Ca^{2+}-free extracellular solution (b), in the Ca^{2+}-free extracellular solution with the continuous hyperpolarizing current injection of −41 pA (*c*) and in recovery (*d*); (B) Superimposed traces of tonic firing in control (*grey line*) and burst firing (*black line*); (C_1) ISI histogram for control; (C_2) ISI histogram for burst firing. Bin width is 59 ms; (D) Burst firing depends on Na^+ current. Burst firing before (*top*) and after treatment with 10 µM riluzole (*bottom*) in a representative DA VTA neuron. Horizontal bars and dashed lines represent the membrane potential of −40 mV.

cellular solution, the firing frequency became 1.7 Hz (**Figure 4(A$_2$)**, d). **Figure 4(B)** shows APs in control and burst-like firing in a faster time scale. In the burst-like firing, a train of spikes rode on a plateau potential and the spike amplitude gradually decreased during the spike train (**Figure 4(B)**). As shown in **Figure 4(C)**, the firing patterns before and after burst-like firing were analyzed by ISI histograms. The ISI is normally distributed with a peak at 590 ms in control (**Figure 4(C$_1$)**, while the ISI histogram skewed leftward with a wider ISI distribution during the burst-like firing (**Figure 4(C$_2$)**. In 11 neurons out of 16 DA VTA neurons (69%), burst-like firing was generated in the Ca^{2+}-free extracellular solution, when continuous hyperpolarizing current was injected (−48.5 ± 5.6 pA); the average CV of firing frequency was 1.62 ± 0.17. The burst-like firing parameters were as follows: burst duration, 826.5 ± 105.2 ms; spike number in the train, 4.9 ± 0.2; ISI, 221.2 ± 18.9 ms; plateau potential, 10.7 ± 0.6 mV (n = 11). As illustrated in **Figure 4(D)**, the burst-like firing induced by the continuous hyperpolarizing current injection in the Ca^{2+}-free extracellular solution was abolished after treatment with 10 μM riluzole; average membrane potential after treatment with riluzole was −62.3 ± 1.4 mV (n = 4).

3.5. Blockade of T-Type Ca^{2+} Channels and SK Channels Did Not Induce Burst Firing

In Ca^{2+}-free extracellular solution, reduced Ca^{2+} influx through voltage-dependent Ca^{2+} channels decreases Ca^{2+}-activated K^+ currents. If this occurred in DA VTA neurons, the counter effect of SK currents would oppose decreases in the depolarizing driving force and burst firing may be induced as previously described in midbrain dopamine neurons [28] [29]. To represent the condition of blocking both voltage-dependent Ca^{2+} current and SK current in Ca^{2+}-free extracellular solution, we used nickel to produce concurrent blockade of T-type Ca^{2+} channels and SK channels, since these two ion channels are strongly coupled in midbrain dopamine neurons [30]. We ascertain that blockade of SK channels by 200 n Mapamin reduced AHP in DA VTA neurons (**Figure 5(A)**). In

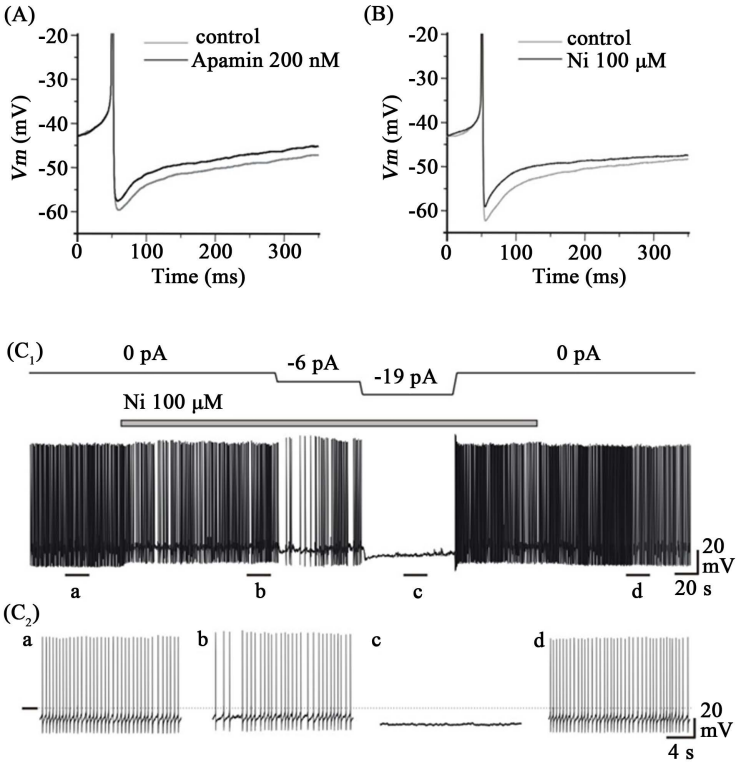

Figure 5. The effects of Ni^{2+} on the firing of DA VTA neurons. (A) Average 10 of APs before (*grey line*) and during apamin treatment without current injection (*black line*). APs are superimposed; (B) Average 10 of APs before (*grey line*) and during nickel treatment without current injection (*black line*); (C_1) Membrane activity before, during and after the application of 100 μM Ni^{2+} with or without continuous hyperpolarizing current injection in a representative DA VTA neuron; (C_2) 20-s segments from the longer record shown in C_1. Firing patterns in the control (a), with 100 μM nickel (b), with 100 μM Ni^{2+} and the continuous hyperpolarizing current injection of −19 pA (c) and in recovery (d). A horizontal bar and a dashed line represent the membrane potential of −40 mV.

a similar manner, Ni^{2+} (100 μM) reduced AHP, which is attributable to SK currents (**Figure 5(B)**). Before nickel treatment, the spontaneous firing frequency was 1.7 Hz (**Figure 5(C_2)**, a). The firing frequency was decreased and firing pattern became irregular in the presence of 100 μM Ni^{2+} (**Figure 5(C_2)**, b). When a continuous hyperpolarizing current was injected during nickel treatment, the firing frequency was decreased and abolished without inducing burst firing (**Figure 5(C_2)**, c). After the continuous hyperpolarizing current injection was removed and Ni^{2+} was washed out, the spontaneous firing frequency became 1.6 Hz (**Figure 5(C_2)**, d). In 5 DA VTA neurons, continuous hyperpolarizing current injection with nickel treatment failed to generate burst firing; the average continuous hyperpolarizing current was −20.0 ± 3.5 pA.

4. Discussion

In our voltage-clamp analysis, the persistent Na^+ current, which was TTX- and riluzole-sensitive, was activated at −60 mV and reached a maximal amplitude at −40 mV in DA VTA neurons. Previous studies have reported that TTX- and riluzole-sensitive persistent Na^+ currents are activated at membrane potentials positive to −60 mV in suprachiasmic nucleus neurons [52], dorsal column nucleus neurons [40], and neocortex neurons [53]. In our current-clamp analysis, blockade of Na^+ current with TTX or riluzole caused membrane hyperpolarization and blocked AP generation in DA VTA neurons. Our findingsindicate that persistent Na^+ current is activated at subthreshold membrane potentials and has a critical role in AP generation in DA VTA neurons, supporting the findings of a previous study in midbrain dopamine neurons [42].

In the present study, the Ca^{2+}-free extracellular solution potentiated persistent Na^+ currents by a negative shift of the activation voltage by 3.5 mV without changing the slope factor, indicating that persistent Na^+ current in the Ca^{2+}-free extracellular solution can be activated by negative membrane potentials between −63.5 mV and −43.5 mV. It is known that extracellular Ca^{2+}reductions potentiate persistent Na^+ currents and this contributes to burst firing [46] [47]. In our current study, burst-like firing induced by the Ca^{2+}-free extracellular solution was completely prevented with 10 μM riluzole, suggesting that the Na^+ current is a major depolarizing driving force in these neurons. We found that concurrent blockade of both T-type Ca^{2+} channels andSK channels by 100 μM Ni^{2+} did not induce burst-like firing in DA VTA neurons. In the presence of nickel, continuous hyperpolarizing current of −20 pA was able to stop AP generation completely. The burst-like firing of DA VTA neurons in Ca^{2+}-free extracellular solution may be induced by a different mechanism from the reduction of SK currents. This is confirmed by comparing properties of Na^+ current-dependent burst-like firing in the current study and those of burst firing induced by the inhibition of SK channels with apamin [28]. The Na^+ current-dependent burst-like firing in the present study had short-term spindle-like plateau with small number of APs during the burst, whereas burst firing induced by SK channel inhibition has long-term ramp-like plateau with greater number of APs during the burst [28].

It is useful to compare the properties of Na^+ current-dependent burst-like firing observed in the present study and Ca^{2+}-dependent carbachol-induced burst firing in DA VTA neurons [27]. For Na^+ current-dependent burst-like firing parameters, the average burst duration was 827 ms, average spike number per burst was 4.9, and average ISI within the burst was 221 ms. Conversely, L-type Ca^{2+} current-dependent burst firing induced by carbachol has a longer burst duration (5 - 10 s), a larger number of spikes (more than 10 during the burst) and a longer ISI within the burst (599 ms) [27]. Another difference between Na^+ current-dependent and Ca^{2+}-dependent carbachol-induced burst firings is a difference in plateau potentials: a spindle-like plateau potential in Na^+ current-dependent burst-like firing and a slowly depolarizing plateau-like potential which lasts for 5 - 10 s in Ca^{2+} current-dependent burst firing [27]. In midbrain dopamine neurons, burst firing induced by the activation of NMDA receptors [22] and by blockade of SK channels with the activation of metabotropic glutamate receptors [29] have similarities with the Ca^{2+} current-dependent burst firing induced by carbachol [27]. Na^+ current-dependent burst-like firing in the present study has similarities with findings of a previous study using brain slice preparations, in which average spike number per burst is 3.7 and average ISI within the burst is 73 ms [18].

A previous study has reported that the concurrent blockade of both T-type Ca^{2+} currents and SK currents with 100 μM Ni^{2+} induced burst firing in a subset of midbrain dopamine neurons [30], whereas 100 μM Ni^{2+} failed to induce burst firing in the present study. The differences between our findings and those of previous studies may depend on experimental preparations, brain slices, and acutely dissociated neurons. In midbrain dopamine neurons from brain slice preparations, Ca^{2+} current-mediated SOPs (0.5 - 1.0 Hz), which underlie the generation of spontaneous firing, are prominent and spontaneous Ca^{2+} spikesare generated by Na^+ current blockade in some

neuronal populations [24] [25]. In dissociated DA VTA neurons, the amplitude of the SOPs was not prominent (<5 mV) (**Figure 1**), suggesting that the Ca^{2+} current contribution to the depolarizing driving force is small in these dissociated neurons. In brain slice preparations, it is likely that Ca^{2+} currentscontribute to AP generation and Na^{+} currents supportAP generation. In addition, SK currents counter the Ca^{2+} current-mediated depolarizing driving force to prevent midbrain dopamine neurons from burst firing in brain slice preparations.

In the present study, the burst-like firing was induced in the dissociated DA VTA neurons under the blockade of Ca^{2+} channels and the elimination of presynaptic effects on these neurons, however, there is a potential limitation in the experimental design of the study. The burst firing was induced by a non-physyological maneuver such as the elimination of extracellular Ca^{2+} with hyperpolarizing current injection. Our findings present a possible biophysiological model for burst firing in DA VTA neurons and suggest that both Na^{+} current- and Ca^{2+} current-dependent intrinsic ionic mechanisms contribute to burst firing in these neurons. Future work will be necessary to delineate the physiological contribution of these ionic currents to burst firing that increases dopamine transmission more effectively in the mesoaccumbal regions in association with accelerated mediation of reinforcing process.

Acknowledgements

This work was supported by National Institute on Alcohol Abuse and Alcoholism Grant AA05846 (to S.B.A.). This study was partly supported by Grants-in-Aid for Scientific Research (C) (Nos. 22500685 and 25350166 to S.K.) from the Japan Society for the Promotion of Science (JSPS) and the Mishima Kaiun Memorial Foundation, Japan (to S.K.). This study was also supported by funds (No. 106006 to S.K.) from the General Research Institute of Fukuoka University.

Competing Interests

The authors have no competing interests to declare.

References

[1] Oades, R.D. and Halliday, G.M. (1987) Ventral tegmental (A10) System: Neurobiology. 1. Anatomy and Connectivity. *Brain Research*, **434**, 117-165. http://dx.doi.org/10.1016/0165-0173(87)90011-7

[2] Appel S.B., McBride, W.J., Diana, M., Diamond, I., Bonci, A. and Brodie, MS. (2004) Ethanol Effects on Dopaminergic "Reward" Neurons in the Ventral Tegmental Area and the Mesolimbic Pathway. *Alcoholism: Clinical and Experimental Research*, **28**, 1768-1778. http://dx.doi.org/10.1097/01.ALC.0000145976.64413.21

[3] McBride, W.J., Murphy, J.M. and Ikemoto, S. (1999) Localization of Brain Reinforcement Mechanisms: Intracranial Self-Administration and Intracranial Place-Conditioning Studies. *Behavioural Brain Research*, **101**, 129-152. http://dx.doi.org/10.1016/S0166-4328(99)00022-4

[4] Robinson, T.E. and Berridge, K.C. (2003) Addiction. *Annual Review of Psychology*, **54**, 25-53. http://dx.doi.org/10.1146/annurev.psych.54.101601.145237

[5] Wise, R.A. (2002) Brain Reward Circuitry: Insights from Unsensed Incentives. *Neuron*, **36**, 229-240. http://dx.doi.org/10.1016/S0896-6273(02)00965-0

[6] Brodie, M.S., Pesold, C. and Appel, S.B. (1999) Ethanol Directly Excites Dopaminergic Ventral Tegmental Area Reward Neurons. *Alcoholism*: *Clinical and Experimental Research*, **11**, 1848-1852. http://dx.doi.org/10.1111/j.1530-0277.1999.tb04082.x

[7] Johnson, S.W. and North, R.A. (1992) Two Types of Neurone in the Rat Ventral Tegmental Area and Their Synaptic Inputs. *Journal of Physiology* (*London*), **450**, 455-468. http://dx.doi.org/10.1113/jphysiol.1992.sp019136

[8] Koyama, S. and Appel, S.B. (2006) Characterization of M-Current in Ventral Tegmental Area Dopamine Neurons. *Journal of Neurophysiology*, **96**, 535-544. http://dx.doi.org/10.1152/jn.00574.2005

[9] Koyama, S., Kanemitsu, Y. and Weight, F.F. (2005) Spontaneous Activity and Properties of Two Types of Principal Neurons from the Ventral Tegmental Area of Rat. *Journal of Neurophysiology*, **93**, 3282-3293. http://dx.doi.org/10.1152/jn.00776.2004

[10] Neuhoff, H., Neu, A., Liss, B. and Roeper, J. (2002) I_h Channels Contribute to the Different Functional Properties of Identified Dopaminergic Subpopulations in the Midbrain. *Journal of Neuroscience*, **22**, 1290-1302.

[11] Gonon, F.G. (1988) Nonlinear Relationship between Impulse Flow and Dopamine Released by Rat Midbrain Dopaminergic Neurons as Studied by *in Vivo* Electrochemistry. *Neuroscience*, **24**, 19-28.

http://dx.doi.org/10.1016/0306-4522(88)90307-7

[12] Chiodo, L.A., Bannon, M.J., Grace, A.A., Roth, R.H. and Bunney, B.S. (1984) Evidence for the Absence of Impulse-Regulating Somatodendritic and Synthesis-Modulating Nerve Terminal Autoreceptors on Subpopulations of Mesocortical Dopamine Neurons. *Neuroscience*, **12**, 1-16. http://dx.doi.org/10.1016/0306-4522(84)90133-7

[13] Kiyatkin, E.A. and Rebec, G.V. (1998) Heterogeneity of Ventral Tegmental Area Neurons: Single-Unit Recording and Iontophoresis in Awake, Unrestrained Rats. *Neuroscience*, **85**, 1285-1309. http://dx.doi.org/10.1016/S0306-4522(98)00054-2

[14] Hyland, B.I., Reynolds, J.N., Hay, J., Perk, C.G. and Miller, R. (2002) Firing Modes of Midbrain Dopamine Cells in the Freely Moving Rat. *Neuroscience*, **114**, 475-492. http://dx.doi.org/10.1016/S0306-4522(02)00267-1

[15] Chergui, K., Suaud-Chagny, M.F. and Gonon, F. (1994) Nonlinear Relationship between Impulse Flow, Dopamine Release and Dopamine Elimination in the Rat Brain *in Vivo*. *Neuroscience*, **62**, 641-645. http://dx.doi.org/10.1016/0306-4522(94)90465-0

[16] Garris, P.A., Ciolkowski, E.L., Pastore, P. and Wightman, R.M. (1994) Efflux of Dopamine from the Synaptic Cleft in the Nucleus Accumbens of the Rat Brain. *Journal of Neuroscience*, **14**, 6084-6093.

[17] Grace, A.A. (1987) The Regulation of Dopamine Neuron Activity as Determined by *in Vivo* and *in Vitro* Intracellular Recordings. In: Chiodo, L.A. and Freeman, A.S., Eds., *Neurophysiology of Dopaminergic Systems—Current Status and Clinical Perspectives*, Lakeshore Publishing Company, Detroit, 1-66.

[18] Grace, A.A. and Bunney, B.S. (1984) The Control of Firing Pattern in Nigral Dopamine Neurons: Burst Firing. *Journal of Neuroscience*, **4**, 2877-2890.

[19] Carr, D.B. and Sesack, S.R. (2000) Projections from the Rat Prefrontal Cortex to the Ventral Tegmental Area: Target Specificity in the Synaptic Associations with Mesoaccumbens and Mesocortical Neurons. *Journal of Neuroscience*, **20**, 3864-3873.

[20] Johnson, S.W., Seutin, V. and North, R.A. (1992) Burst Firing in Dopamine Neurons Induced by *N-Methyl-D-Aspartate*: Role of Electrogenic Sodium Pump. *Science*, **258**, 665-667. http://dx.doi.org/10.1126/science.1329209

[21] Mereu, G., Lilliu, V., Casula, A., Vargiu, P.F., Diana, M., Musa, A. and Gessa, G.L. (1997) Spontaneous Bursting Activity of Dopaminergic Neurons in Midbrain Slices from Immature Rats: Role of *N-Methyl-D-Aspartate* Receptors. *Neuroscience*, **77**, 1029-1036. http://dx.doi.org/10.1016/S0306-4522(96)00474-5

[22] Paladini, C.A., Iribe, Y. and Tepper, J.M. (1999) $GABA_A$ Receptor Stimulation Blocks NMDA-Induced Bursting of Dopaminergic Neurons *in Vitro* by Decreasing Input Resistance. *Brain Research*, **832**, 145-151. http://dx.doi.org/10.1016/S0006-8993(99)01484-5

[23] Wang, T., O'Connor, W.T., Ungerstedt, U. and French, E.D. (1994) *N-Methyl-D-Aspartic* Acid Biphasically Regulates the Biochemical and Electrophysiological Response of A10 Dopamine Neurons in the Ventral Tegmental Area: *In Vivo* Microdialysis and *in Vitro* Electrophysiological Studies. *Brain Research*, **666**, 255-262. http://dx.doi.org/10.1016/0006-8993(94)90780-3

[24] Fujimura, K. and Matsuda, Y. (1989) Autogenous Oscillatory Potentials in Neurons of the Guinea Pig Substantia Nigra Pars Compacta *in Vitro*. *Neuroscience Letters*, **104**, 53-55. http://dx.doi.org/10.1016/0304-3940(89)90328-5

[25] Kang, Y. and Kitai, S.T. (1993) Calcium Spike Underlying Rhythmic Firing in Dopaminergic Neurons of the Rat Substantia Nigra. *Neuroscience Research*, **18**, 195-207. http://dx.doi.org/10.1016/0168-0102(93)90055-U

[26] Nedergaard, S., Flatman, J.A. and Engberg, I. (1993) Nifedipine- and ω-Conotoxin-Sensitive Ca^{2+} Conductances in Guinea-Pig Substantia Nigra Pars Compacta Neurones. *Journal of Physiology*, **466**, 727-747.

[27] Zhang, L., Liu, Y. and Chen, X. (2005) Carbachol Induces Burst Firing of Dopamine Cells in the Ventral Tegmental Area by Promoting Calcium Entry through L-Type Channels in the Rat. *Journal of Physiology*, **568**, 469-481. http://dx.doi.org/10.1113/jphysiol.2005.094722

[28] Ping, H.X. and Shepard, P.D. (1996) Apamin-Sensitive Ca^{2+}-Activated K^+ Channels Regulate Pacemaker Activity in Nigral Dopamine Neurons. *NeuroReport*, **7**, 809-814. http://dx.doi.org/10.1097/00001756-199602290-00031

[29] Prisco, S., Natoli, S., Bernardi, G. and Mercuri, N.B. (2002) Group I Metabotropic Glutamate Receptors Activate Burst Firing in Rat Midbrain Dopaminergic Neurons. *Neuropharmacology*, **42**, 289-296. http://dx.doi.org/10.1016/S0028-3908(01)00192-7

[30] Wolfart, J. and Roeper, J. (2002) Selective Coupling of T-Type Calcium Channels to SK Potassium Channels Prevents Intrinsic Bursting in Dopaminergic Midbrain Neurons. *Journal of Neuroscience*, **22**, 3404-3413.

[31] Agrawal, N., Hamam, B.N., Magistretti, J., Alonso, A. and Ragsdale, D.S. (2001) Persistent Sodium Channel Activity Mediates Subthreshold Membrane Potential Oscillations and Low-Threshold Spikes in Rat Entorhinal Cortex Layer V Neurons. *Neuroscience*, **102**, 53-64. http://dx.doi.org/10.1016/S0306-4522(00)00455-3

[32] Alonso, A. and Llinas, R.R. (1989) Subthreshold Na^+-Dependent Theta-Like Rhythmicity in Stellate Cells of Entor-

hinal Cortex Layer II. *Nature*, **342**, 175-177. http://dx.doi.org/10.1038/342175a0

[33] Chapman, C.A. and Lacaille, J.C. (1999) Intrinsic Theta-Frequency Membrane Potential Oscillations in Hippocampal CA1 Interneurons of Stratum Lacunosum-Moleculare. *Journal of Neurophysiology*, **81**, 1296-1307.

[34] Jinno, S., Ishizuka, S. and Kosaka, T. (2003) Ionic Currents Underlying Rhythmic Bursting of Ventral Mossy Cells in the Developing Mouse Dentate Gyrus. *European Journal of Neuroscience*, **17**, 1338-1354. http://dx.doi.org/10.1046/j.1460-9568.2003.02569.x

[35] Pape, H.C., Pare, D. and Driesang, R.B. (1998) Two Types of Intrinsic Oscillations in Neurons of the Lateral and Basolateral Nuclei of the Amygdala. *Journal of Neurophysiology*, **79**, 205-216.

[36] Bracci, E., Centonze, D., Bernardi, G. and Calabresi, P. (2003) Voltage-Dependent Membrane Potential Oscillations of Rat Striatal Fast-Spiking Interneurons. *Journal of Physiology*, **549**, 121-130. http://dx.doi.org/10.1113/jphysiol.2003.040857

[37] Boehmer, G., Greffrath, W., Martin, E. and Hermann, S. (2000) Subthreshold Oscillation of the Membrane Potential in Magnocellular Neurones of the Rat Supraoptic Nucleus. *Journal of Physiology*, **526**, 115-128. http://dx.doi.org/10.1111/j.1469-7793.2000.t01-1-00115.x

[38] Taddese, A. and Bean, B.P. (2001) Subthreshold Sodium Current from Rapidly Inactivating Sodium Channels Drives Spontaneous Firing of Tuberomammillary Neurons. *Neuron*, **33**, 587-600.

[39] Wu, N., Hsiao, C.F. and Chandler, S.H. (2001) Membrane Resonance and Subthreshold Membrane Oscillations in Mesencephalic V Neurons: Participants in Burst Generation. *Journal of Neuroscience*, **21**, 3729-3739.

[40] Reboreda, A., Sanchez, E., Romero, M. and Lamas, J.A. (2003) Intrinsic Spontaneous Activity and Subthreshold Oscillations in Neurones of the Rat Dorsal Column Nuclei in Culture. *Journal of Physiology*, **551**, 191-205. http://dx.doi.org/10.1113/jphysiol.2003.039917

[41] Amir, R., Michaelis, M. and Devor, M. (1999) Membrane Potential Oscillations in Dorsal Root Ganglion Neurons: Role in Normal Electrogenesis and Neuropathic Pain. *Journal of Neuroscience*, **19**, 8589-8596.

[42] Puopolo, M., Raviola, E. and Bean, B.P. (2007) Roles of Subthreshold Calcium Current and Sodium Current in Spontaneous Firing of Mouse Midbraine Dopamine Neurons. *Journal of Neuroscience*, **27**, 245-656. http://dx.doi.org/10.1523/JNEUROSCI.4341-06.2007

[43] Astma, N., Gutnick, M.J. and Fleidervish, I.A. (1998) Activation of Protein Kinase C Increases Neuronal Excitability by Regulating Persistent Na^+ Current in Mouse Neocortical Slices. *Journal of Neurophysiology*, **80**, 1547-1551.

[44] Franceschetti, S., Taverna, S., Sancini, G., Panzica, F., Lombardi, R. and Avanzini, G. (2000) Protein Kinase C-Dependent Modulation of Na^+ Currents Increases the Excitability of Rat Neocortical Pyramidal Neurones. *Journal of Physiology*, **528**, 291-304. http://dx.doi.org/10.1111/j.1469-7793.2000.00291.x

[45] Pena, F. and Ramirez, J.M. (2002) Endogenous Activation of Serotonin-2A Receptors Is Required for Respiratory Rhythm Generation *in Vitro*. *Journal of Neuroscience*, **22**, 11055-11064.

[46] Mantegazza, M., Franceschetti, S. and Avanzini, G. (1998) Anemone Toxin (ATX II)-Induced Increase in Persistent Sodium Current: Effects on the Firing Properties of Rat Neocortical Pyramidal Neurones. *Journal of Physiology*, **507**, 105-116. http://dx.doi.org/10.1111/j.1469-7793.1998.105bu.x

[47] Shuai, J., Bikson, M., Hahn, P.J., Lian, J. and Durand, D.M. (2003) Ionic Mechanisms Underlying Spontaneous CA1 Neuronal Firing in Ca^{2+}-Free Solution. *Biophysical Journal*, **84**, 2099-2111. http://dx.doi.org/10.1016/S0006-3495(03)75017-6

[48] Su, H., Alroy, G., Kirson, E.D. and Yaari, Y. (2001) Extracellular Calcium Modulates Persistent Sodium Current-Dependent Burst-Firing in Hippocampal Pyramidal Neurons. *Journal of Neuroscience*, **21**, 4173-4182.

[49] Neher, E. (1992) Correction for Liquid Junction Potential in Patch Clamp Experiments. *Methods in Enzymology*, **207**, 123-131. http://dx.doi.org/10.1016/0076-6879(92)07008-C

[50] Brodie, M.S., Shefner, S.A. and Dunwiddie, T.V. (1990) Ethanol Increases the Firing Rate of Dopamine Neurons of the Ventral Tegmental Aria *in Vitro*. *Brain Research*, **508**, 65-69. http://dx.doi.org/10.1016/0006-8993(90)91118-Z

[51] Cocatre-Zilgien, J.H. and Delcomyn, F. (1992) Identification of Bursts in Spike Trains. *Journal of Neuroscience and Methods*, **41**, 19-30. http://dx.doi.org/10.1016/0165-0270(92)90120-3

[52] Kononenko, N.I., Shao, L.R. and Dudek, F.E. (2004) Riluzole-Sensitive Slowly Inactivating Sodium Current in Rat Suprachiasmatic Nucleus Neurons. *Journal of Neurophysiology*, **91**, 710-718. http://dx.doi.org/10.1152/jn.00770.2003

[53] Urbani, A. and Belluzzi, O. (2000) Riluzole Inhibits the Persistent Sodium Current in Mammalian CNS Neurons. *European Journal of Neuroscience*, **12**, 3567-3574. http://dx.doi.org/10.1046/j.1460-9568.2000.00242.x